

Path-overlap Avoidance in Multiple Route Construction for Mobile Relay on WSN

Yogi Anggun Saloko YUDO¹, Noritaka SHIGEI¹, and Hiromi MIYAJIMA¹

¹Graduate School of Science and Engineering, Kagoshima University

Abstract

ENERGY is the most important resource in Wireless Sensor Network (WSN) [1], because it determines the lifetime of a sensor node. Since the sensor nodes are usually powered by limited power batteries, low energy consumption is very important, in order to prolong the network lifetime of WSN. In recent years, many researchers designed and developed techniques for prolonging the network lifetime of WSN [1,2]. One of the techniques is mobile relay [3,4,5]. The concept of mobile relay is that some movable nodes change their location so as to minimize the total energy consumed by both wireless transmission and locomotion. Mobile relay needs to determine an initial route, which describes the sequence of nodes used for relaying the data from a source node to a sink node, and then the relaying nodes change their location so as to reduce their energy consumption.

In previous studies, we have already proposed Battery-Aware Initial Route Construction-Dijkstra's algorithm (BAIR-D) for determining the initial route based on Dijkstra's algorithm [6]. This method can construct the optimal path in terms of given cost function. Further, the algorithm takes into account nodes' battery levels and avoids using nodes with low battery levels. However, when applying it to multiple sources, a problem arises. Since BAIR-D constructs the optimal path for each source, the constructed paths are necessarily overlapped with a high probability. The path-overlap increases the energy consumption of the nodes on overlapped paths. This makes the overloaded nodes go quickly down.

In this paper, we propose battery-aware multiple route construction with path-overlap avoidance (BMRC-POA). To overcome the problem in the conventional method, BMRC-POA finds the initial route for mobile relay with path-overlap avoidance. It avoids some nodes to be a relaying node for multiple source nodes. It also avoids the source node to be a relaying node to another source node. Avoiding path-overlap in multiple route construction can save the energy for some sensor nodes. Therefore, it can prolong the lifetime of sensor nodes. This method consists of two steps. First, the initial route construction for every source node is determined without path-overlap. Second, if some source nodes have no route, then the initial route construction is performed with a path-overlap scenario. We compare BMRC-POA and BAIR-D in terms of the number of operating rounds and the successful rate of initial route construction. Further, we compare both of the methods in terms of the total cost. The effectiveness of BMRC-POA is demonstrated by using numerical simulation.

References

- 1) J. Yick, B. Mukherjee and D. Ghosal, "Wireless Sensor Network Survey", *Computer Networks*, Vol. 52, pp. 2292-2330, 2008.
- 2) C.Hua and T. P. Yum, "Optimal routing and data aggregation for maximizing lifetime of wireless sensor networks," *IEEE ACM Trans, Netw.*, vol.16, no. 4, pp. 892-903, 2008.
- 3) F. El-Moukaddem, E. Torng, G. Xing and S. Kulkarni, "Mobile Relay Configuration in Data-intensive Wireless Sensor Networks", *Proc. of Int. Conf. on Mobile Adhoc and Sensor Systems*, pp. 80-89, 2009.
- 4) F. El-Moukaddem, E. Torng, and G.Xing, "Maximing Data Gathering Capacity if Wireless Sensor Networks using Mobile Relays", *Proc. of Int. Conf. on Mobile Adhoc and Sensor Systems*, pp.312-321, 2010.
- 5) N. Shigei, I. Fukuyama, H. Miyajima and Yogi A. Saloko Yudo, "Battery-Aware Algorithm for Mobile Relay and Route Construction on Wireless Sensor Network", *IAENG Int. Journal of Computer Science*, vol. 39, no. 3, pp. 321-328, 2012.
- 6) Yogi A. Saloko Yudo, N. Shigei and H. Miyajima, "Effective Initial Route Construction for Mobile Relay on Wireless Sensor Network", *Proc. of Int. Symposium on Artificial Life and Robotic*, pp.311-316, 2014.

On the Capability of a Fuzzy Inference System With Improved Interpretability

Hirofumi MIYAJIMA¹, Noritaka SHIGEI¹ and Hiromi MIYAJIMA¹

¹Graduate School of Science and Engineering, Kagoshima University

Abstract

Many studies on modeling of fuzzy inference systems have been made. The issue of these studies is to construct automatically fuzzy systems with interpretability and accuracy from learning data based on meta-heuristic methods[1]. Since accuracy and interpretability are contradicting issues, there are some disadvantages for self-tuning method[2]. Obvious drawbacks of the method are lack of interpretability and getting stuck in a shallow local minimum. Therefore, the conventional learning methods with multi-objective fuzzy modeling and fuzzy modeling with constrained parameters of the ranges have become popular. However, there are little studies on effective learning methods of fuzzy inference systems dealing with interpretability and accuracy. In this paper, we will propose a fuzzy inference system with interpretability. Firstly, it is proved that the proposed model is an universal approximator of continuous functions[3]. Further, the capability of the proposed model learned by the steepest descend method is compared with the conventional models using function approximation problems. Lastly, the proposed model is applied to obstacle avoidance and the capability of interpretability is shown[4].

Reference

- 1) H. Nomura, I. Hayashi and N. Wakami, A Learning Method of Simplified Fuzzy Reasoning by Genetic Algorithm, Proc. of the Int. Fuzzy Systems and Intelligent Control Conference, pp.236-245, 1992.
- 2) M. J. Gacto, R. Alcalá and F. Herrera, Interpretability of Linguistic Fuzzy Rule-based Systems: An Overview of Interpretability Measures, Inf. Sciences 181, pp.4340-4360, 2011.
- 3) M.M. Gupta, L. Jin and N. Homma, Static and Dynamic Neural Networks, IEEE Press, 2003.
- 4) H. Miyajima, N. Shigei and H. Miyajima, An Application of Fuzzy Inference System Composed of Double-Input Rule Modules to Control Problems, Proceedings of the International MultiConference of Engineers and Computer Scientists 2014 Vol I, IMECS 2014, March 12-14, 2014.

SIMULTANEOUS DEBLUR AND SUPER-RESOLUTION TECHNIQUE FOR VIDEO SEQUENCE CAPTURED BY HAND-HELD VIDEO CAMERA

Yuki MATSUSHITA¹, Hiroshi KAWASAKI¹, Shintaro ONO² and Katsushi IKEUCHI²

¹ Graduate School of Science and Engineering, Kagoshima University

² Institute of Industrial Science, University of Tokyo

Abstract

Nowadays, video camera is commonly used everywhere and demand of retrieving a single shot from video sequence is increasing[1][2][3]. Since resolution of video camera is usually lower than that of digital camera, simply cutting out a frame from a video sequence ends up with low quality. Further, because of the necessity of high fps on video camera, video data inevitably contains motion blur and it leads mis-registration between frames which is critical for multi-frame super-resolution. In this paper, we propose a method to restore high-resolution image from a video sequence considering motion blur. Since the frame-rate of a video camera is high, motion of the object in successive frames is small, and thus, stable feature tracking during short sequences is possible even if there is a blur.[4][5] Thus, we adopt a division/integration approach to realize robust tracking for long sequence. We also propose a simultaneous deblur and super-resolution technique using multiple images based on MAP estimation.

Experimental results are shown to prove the strength of our method. (Figure.1)



Figure 1. Real scene experimental results.

References

- 1) Sunghyun Cho, Jue Wang, and Seungyong Lee, "Video deblurring for hand-held cameras using patch-based synthesis," *ACM Transactions on Graphics*, vol. 31, no.4, pp. 64:1–64:9, 2012.
- 2) Yunpeng Li, Sing Bing Kang, Neel Joshi, Steven M. Seitz, and Daniel P. Huttenlocher, "Generating sharp panoramas from motion-blurred videos," in *CVPR*, 2010, pp. 2424–2431.
- 3) Tae Hyun Kim, Byeongjoo Ahn, and Kyoung Mu Lee, "Dynamic scene deblurring," December 2013.
- 4) Ville Ojansivu and Janne Heikkilä, "Image registration using blur-invariant phase correlation," *IEEE Signal Process. Lett.*, vol. 14, no. 7, pp. 449–452, 2007.
- 5) Sei Nagashima, Takafumi Aoki, Tatsuo Higuchi, and Koji Kobayashi, "A subpixel image matching technique using phase-only correlation," in *Intelligent Signal Processing and Communications, 2006. ISPACS'06. International Symposium on*. IEEE, 2006, pp. 701–704.

Total Temperature Measurement of Gas Flow in Micro-tube with Constant Wall Temperature

Seiryu MATSUSHITA¹, Taiki NAKAMURA¹, Chungpyo HONG¹ and Yutaka ASAKO²

¹Graduate School of Science and Engineering, Kagoshima University
²Dept. of Mechanical Eng., Tokyo Metropolitan University,

Abstract

This paper describes experimental results on total temperature measurement of nitrogen micro-jet from micro-tubes outlet measured for the wide range from unchoked to choked flow. The experiments were performed for a stainless micro-tube of 523.2 μm in diameter whose temperature difference between the wall and inlet was maintained at 2, 5 and 10 K by circulating water around the micro-tube, respectively (Fig. 1). The gas flows out to the atmospheric condition. A thermally insulated tube of foamed polystyrene with six baffles fabricated by the companion paper where the gas velocity reduces and the kinetic energy is converted into the thermal energy, was attached to the outlet of the micro-tube. The inner diameter of the polystyrene tube is 22 mm. The baffles are equally spaced and the intervals of the baffles tested are 5 and 10 mm to investigate the effect of the interval of the baffle on the reduction of the gas velocity. The gas temperature measured by thermocouples at locations of baffles is considered as total temperature. The measured total temperature is higher than the wall temperature and increases with increasing the stagnation pressure (Reynolds number) for unchoked flow since the additional heat transfer from the wall to the gas near the micro-tube outlet caused by the temperature fall due to the energy conversion into the kinetic energy. It decreases in the insulated tube for choked flow since Joule-Thomson effect is dominant in the insulated tube. The measured total temperatures are compared with results obtained by numerical computations (Fig. 2).

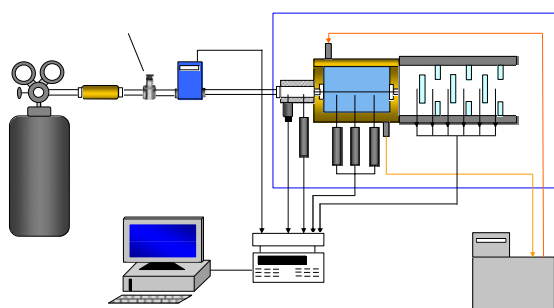


Fig. 1 Schematic of experimental setup

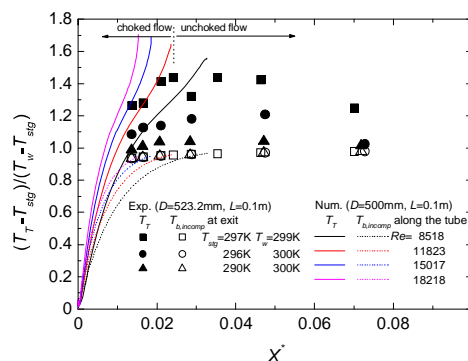


Fig. 2 Normalized total temperature

Interference Analysis of Dual-band WiCoPT System for Wireless Sensor Network in RVT

Ryo TAKAMORI¹, Kenjiro NISHIKAWA¹, Yusuke MARU² and Shigeo KAWASAKI²

¹ Graduate School of Science and Engineering, Kagoshima University

² Japan Aerospace Exploration Agency

Abstract

This paper proposes and demonstrates a dual-band Wireless Communication and Power Transmission (WiCoPT) system for a wireless health monitoring sensor network in Reusable Vehicle Test (RVT). Fig. 1 shows the wireless health monitoring system based on the dual-band WiCoPT. The proposed dual-band WiCoPT system employs 25 GHz-band for uplink and data transfer and 5 GHz-band for downlink and power transfer, resulting in an efficient wireless sensor system. The paper also analyzed the interference between uplink signals and downlink signals on the IC tag. When the interference power level from the downlink is less than 0 dBm on the IC tag, the uplink performances are suitable (Fig. 2). While the stable performance of the downlink are achieved when the interference power level from the base station is less than -25 dBm (Fig. 3). Under the above conditions, each EVM value is less than 10%. In addition, the uplink performances slightly depend on the linearity of the output power amplifier. Those results provide us a design guide to realize the WiCoPT health monitoring system in the RVT.

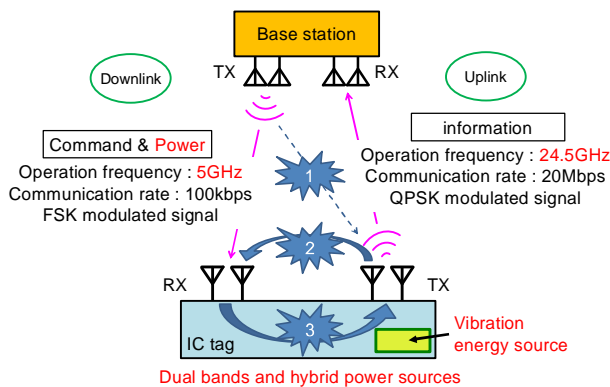


Fig. 1. Dual-band WiCoPT system

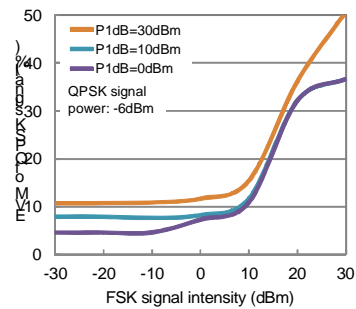


Fig. 2. EVM performances of transmitter.

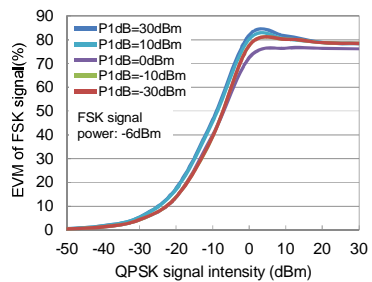


Fig. 3. EVM performances of receiver

Performance Analysis of Adjacent Channel Leakage power Ratio depending on RF Components for Multiband Base Station

Hiroto SAKAKI¹, Masanobu TUSJII¹, Kenjiro NISHIKAWA¹, Kunihiro KAWAI², Hiroshi OKAZAKI², and Shoichi NARAHASHI²

¹ Graduate School of Science and Engineering, Kagoshima University

² Research Laboratory, NTT DOCOMO

Abstract

Future mobile communication systems demanded a carrier aggregation (CA) techniques and a multi-input multi-output (MIMO) transmission system to increase data traffic[1]-[3]. A high linear multiband low-noise amplifier (LNA) is a key component to realize the future systems. This paper analyzes the relationship between the Adjacent Channel Leakage power Ratio (ACLR) and performances of the LNA and band pass-filter in an RF front-end. To achieve -30dBc ACLR, for instance, low linear LNA requires -55 dB out of band suppression BPF to achieve the same ACLR. These results provided a design guidance of the receiver on the mobile base station for system designers.

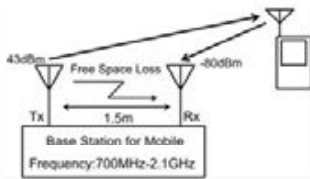


Fig. I System model

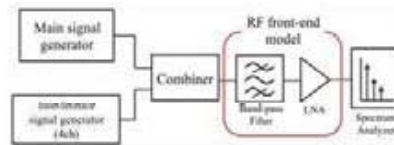
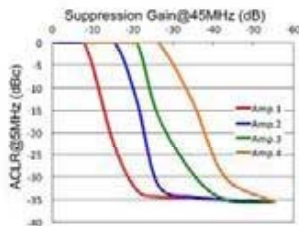
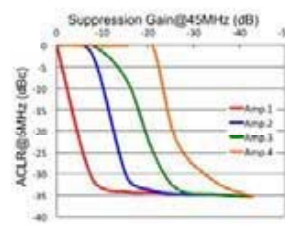


Fig. II Block diagram of Simulation



(a) 700 MHz



(b) 2.1 GHz

Fig. III ACLR versus filter performance

Reference

- 1) R. Ratasuk, D. Tolli, A. Ghosh, "Carrier Aggregation in LTE-Advanced," 2010 IEEE 71st Vehicular Technology Conference, pp. 1-5, May 2010.
- 2) A. Ghosh, R. Ratasuk, B. Mondal, "LTE- Advanced: next-generation wireless broadband technology," IEEE Wireless Communications, pp.10-22, Jun. 2010.
- 3) P.L. Tsai, K.C.J Lin, W.T. Chen, "Downlink radio resource allocation with Carrier aggregation in MIMO LTE-advanced systems," 2014 IEEE Int. Conf. on Communications (ICC), pp. 10-14, Jun. 2014.

Structural Morphogenesis for Grid Shell with Member of Uniform Length and Cross Section by Genetic Algorithms to Implement Manipulation of Decent Solutions Search

Yuto NISHIMORI¹, Toshio HONMA¹ and Yohei YOKOSUKA¹

¹ Graduate School of Science and Engineering, Kagoshima University

Abstract

In this paper, the structural morphogenesis for a grid shell with the members of uniform length and cross section is indicated. The design of the grid shell structure with free curved surface for a large space became realizable from the confirmation of the structural rationality and the improvement in construction technology. However, the constraint for the productivity and constructability of these structures are produced in the length and cross section of the structural members.

In general, an optimization technique is used to obtain the global optimal solution. One of the authors proposed GA with immune system (ISGA) [1] for the structural optimization procedure that implemented the manipulation of the decent solutions search. The decent solutions have comparatively high evaluation value including the global optimal solution and the local optimal solutions and those neighborhood solutions. The decent solutions obtained by ISGA maintain diversity both in the design variable space and the objective function space. This structural optimization procedure with the manipulation of the decent solutions search is applied to structural morphogenesis for the grid shell [2]. The acquisition of the obtained rational and diversified solution forms will be used to support designer's idea.

In the numerical examples, the decent solution forms of the analysis model for the symmetric grid shell structure are shown for an in plane rectangular geometry. First, we indicate the geometric relationship and computational procedure for creating curved surface using Bézier when the structural members are set to a uniform length and cross section. Next, we apply this technique to the structural morphogenesis for a grid shell with single-objective optimization problem for the total strain energy minimization or the bending strain energy minimization. Last, the structural properties of these decent solutions obtained by ISGA containing a global optimal solution and local optimal solutions are verified.

Figure below are some numerical examples of the decent solution forms for the grid shell structure with uniform length of all members. The cross section of the member in these forms has been optimized. In the boundary condition of the analysis model, the corner parts are pinned support.

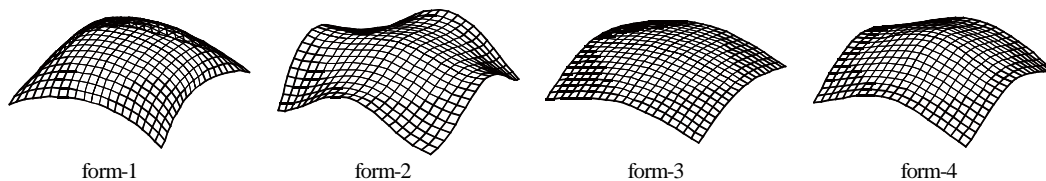


Figure. Decent solution forms with uniform length

References

- 1) T. Honma and K. Nozui : Structural Morphogenesis by using Genetic Algorithms with Diversity of Solution, Journal of structural and construction engineering. Transaction of AIJ, 614, 35-43, 2007. 4 (in Japanese)
- 2) Y. Okita and T. Honma, Structural morphogenesis for free-form grid shell using genetic algorithms with manipulation of decent solution search, Journal of the International Association for Shell and Spatial Structures, 53 (3), 177-184, 2012. 9
- 3) M. Ohsaki and S. Fujita, Multiobjective shape optimization of latticed shells for elastic stiffness and uniform member lengths, Proc. Int. Symposium on Algorithmic Design for Architecture and Urban Design (ALGODE TOKYO 2011), 2011.

Structural Shape Optimization of Free-Form Surface Shell and Property of Solution Search Using Firefly Algorithm

Natsuki TANAKA¹, Toshio HONMA¹ and Yohei YOKOSUKA¹

¹ Graduate School of Science and Engineering, Kagoshima University

Abstract

In the architecture field, structural shape optimization is needed to obtain form with mechanical rationality, and any of the multiple forms obtained by structural optimization can possibly support ideas of designer. Structural shape optimization has the heuristic optimization procedures such as genetic algorithm (GA) and swarm intelligence (SI) in one of the typical solution search techniques. GA is a scheme based on the mechanism of biological evolution. SI is a scheme that uses patterns found in self-organizing phenomena observed in nature. The well-known SI techniques include the particle swarm optimization (PSO), which is based on group behavior of birds and fish [1], and the artificial bee colony (ABC), which is based on the foraging behavior of a honeybee swarm [2], and are applied to a lot of structural optimization. A lot of SI including PSO and ABC attain a global optimal solution, and diversity on the design variable space of those solutions is low. The firefly algorithm (FA) was developed recently as the optimization computational scheme using a firefly's ecology [3]. FA can attain both a global optimal solution and local optimal solutions by setting suitable computational parameters. However, the method for setting these parameters is comparatively difficult because the objective function space differs depending on the optimization problem [4]. In order to simplify the setting of these parameters in FA, we implement the computational scheme where the distance between two fireflies in the design variable space is dimensionless.

In this study, FA is applied to the structural shape optimization of a free-form surface shell. The solution forms that are obtained by FA are compared with those obtained by PSO, ABC and differential evolution (DE) [5]. DE is an evolutionary computational scheme, and performs solution search manner in similar to GA. The forms-1-3 and forms-4-6 that obtained by FA show solution forms that obtained by the total strain and bending strain energy minimization of a free-form surface shell structure, respectively. These solutions are applied to the local search [6] as an initial solution form, and it is indicated that the solution obtained by FA is extremal solution of a high estimation. In this paper, the effectiveness and the validity of FA for structural shape optimization are indicated through these numerical results.

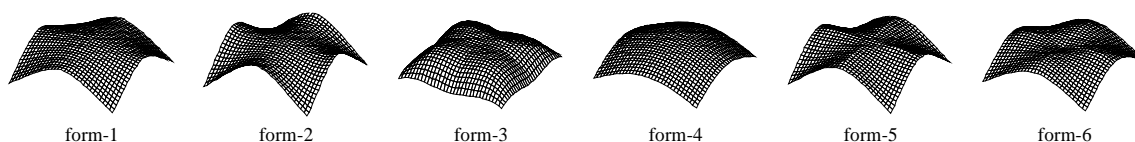


Figure. Example of solution forms of free-form surface shell

References

- 1) J.Kennedy and R.Eberhart, Particle Swarm Optimization, Proc. of IEEE Inter. Conf. on Neural Network, IV (1995) 1942-1948.
- 2) D.Karaboga and B.Basturk, A powerful and efficient algorithm for numerical function optimization: artificial bee colony (ABC) algorithm, Journal of Glob Optimization 39 (2007) 459-471.
- 3) Xin-She Yang, Firefly Algorithms for Multimodal Optimization, Proc. 5th Inter. Conf. on Stochastic Algorithms, Foundations and Applications (2009) 169-178.
- 4) N.Tanaka and T.Honma, Structural Shape Optimization of Free-Form Surface Shell Using Firefly Algorithm, Proc. of IASS Symposium 2013, "BEYOND THE LIMITS OF MAN", CD-ROM1226, 1-8
- 5) R. Storn and K. Price, Differential Evolution - A simple and efficient heuristic for global optimization over continuous spaces, Journal of Glob Optimization 11 (1997) 341-359
- 6) Stuart J. Russell, Peter Norvig, Artificial Intelligence: A Modern Approach, Second edition, Upper Saddle River, New Jersey, Prentice Hall (2002) 111-114.

Preparation of Chitin-based Nanomaterials by Gas Bubbling-Ultrasonic Treatments

Kohei TANAKA, Kazuya YAMAMOTO, Jun-ichi KADOKAWA

Graduate School of Science and Engineering, Kagoshima University

Abstract

Chitin is one of the most abundant biomass resources. Although the construction of nanostructures is an efficient method for chitin materialization [1], they generally tend to aggregate by drying [2]. In this study, we found that nanowire network structures were constructed from chitin derivatives by gas bubbling-ultrasonic treatments in water. Furthermore, we also have paid attention to an amidine group to develop chitin nanowire network with re-construction property because the group reversibly changes to the amidinium bicarbonate under CO₂ atmosphere [3]. When chitin was first subjected to N₂ gas bubbling-ultrasonic treatments in water, the SEM image showed that nanowire network structure was constructed (Figure 1a). Then, a partially deacetylated chitin (PDA-chitin) was prepared by deacetylation of acetamido groups of the product under alkaline conditions [4]. Amidine groups were introduced by the reaction of primary amines in PDA-chitin with *N,N*-dimethylacetamide dimethyl acetal. After the amidinated chitin was subjected to CO₂ gas bubbling-ultrasonic treatments in water, the SEM image showed that nanowire network structure was remained. We examined re-nanostructuralization of the aggregated material, which was obtained by drying under reduced pressure. Consequently, the material was re-nanostructured by ultrasonic treatment in water (Figure 1b). This behavior was probably caused by the electrostatic repulsion of amidinium bicarbonates [5].

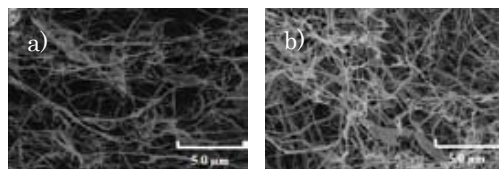


Figure 1. SEM images of chitin after N₂ bubbling and ultrasonic treatments (a) and amidinium chitin after re-nanostructuralization (b).

References

- 1) Y. Fan, T. Saito, A. Isogai, *Biomacromolecules*, 2008, 9, 192–198.
- 2) S. Ifuku, M. Nogi, M. Yoshioka, M. Morimoto, H. Yano, H. Saimoto, *Carbohydr. Polym.*, 2010, 81, 134–139.
- 3) Q. Zhang, W. Wang, Y. Lu, B. Li, S. Zhu, *Macromolecules*, 2011, 44, 6539-6545.
- 4) S. Phougying, S. Aiba, S. Chirachanchai, *Polymer*, 2007, 48, 393-400.
- 5) K. Tanaka, K. Yamamoto, J. Kadokawa, *Carbohydr. Res.*, 2014, 398, 25-30.

Enzymatic Synthesis of Non-natural α -Glucosamine Chains by Thermostable Phosphorylase Catalysis

Riko SHIMOHIGOSHI, Kazuya YAMAMOTO and Jun-ichi KADOKAWA

Graduate School of Science and Engineering, Kagoshima University

Abstract

Phosphorylase is the enzyme that catalyzes phosphorolysis of α -(1 \rightarrow 4)-glucans at a nonreducing end, such as glycogen and amylose, giving α -D-glucose 1-phosphate (Glc-1-P). By means of the reversibility of the reaction, α -(1 \rightarrow 4)-glucans can be prepared by the phosphorylase-catalyzed α -glucosylation using Glc-1-P as a glycosyl donor and a maltooligosaccharide as a glycosyl acceptor [1]. Because of loose specificity for the recognition of substrates [2], phosphorylase recognizes several analogue substrates of Glc-1-P as glycosyl donors in α -glycosylations to give non-natural oligosaccharides. For example, we previously reported that α -D-glucosamine 1-phosphate (GlcN-1-P) could be used as a glycosyl donor in potato phosphorylase-catalyzed enzymatic α -glucosamylation to give oligosaccharides having a glucosamine (GlcN) residue at a nonreducing end [3]. Because it is known that thermostable phosphorylase differs in recognition ability of substrates from potato phosphorylase, in this study, we have examined the thermostable phosphorylase-catalyzed enzymatic α -glucosaminylations using GlcN-1-P (Figure 1). Consequently, we found that successive α -glucosaminylations occurred by thermostable phosphorylase catalysis to give non-natural α -glucosamine chains. When the enzymatic reaction was conducted in ammonia buffer containing Mg^{2+} ion, the α -glucosaminylations were accelerated owing to the precipitation of inorganic phosphate to produce the high molecular weight products.

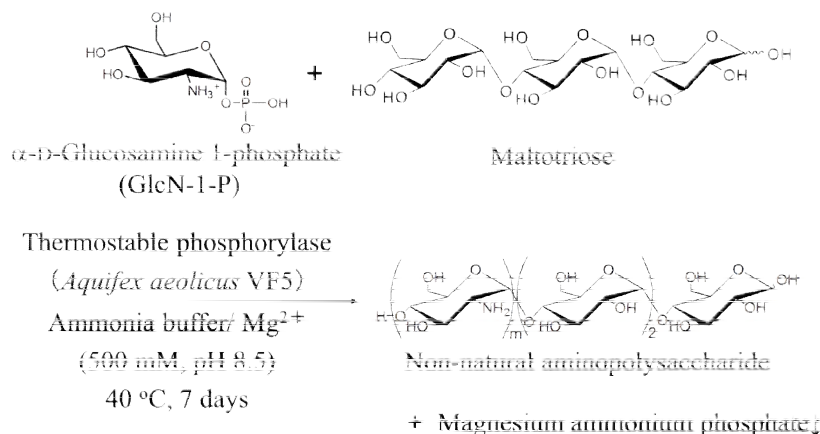


Figure 1. Thermostable phosphorylase-catalyzed successive α -glucosaminylations of maltotriose

References

1. G. Ziegast, B. Pfannemüller, Carbohydr. Res., 160, 185 (1987).
2. J. Kadokawa, Trends Glycosci. Glycotechnol., 25, 57 (2013).
3. M. Nawaji, H. Izawa, Y. Kaneko, J. Kadokawa, Carbohydr. Res., 343, 2692 (2008).

Preparation of Inclusion Supramolecular Polymers by Vine-twining Polymerization Approach

Shota SASAYAMA¹, Kazuya YAMAMOTO¹, Tomonari TANAKA², Yoshiharu KIMURA²,
Jun-ichi KADOKAWA¹

¹ Graduate School of Science and Engineering, Kagoshima University

² Graduate School of Science and Technology, Kyoto Institute of Technology

Abstract

Amylose is a polysaccharide with helical conformation linked through $\alpha(1\rightarrow4)$ -glycosidic linkages. It is a well-known host compound that forms inclusion complexes with hydrophobic guest compounds having relatively lower molecular weight. However, little has been reported regarding the formation of inclusion complexes between amylose and polymeric compounds. In the previous studies, we have developed a new methodology for the preparation of inclusion complexes composed of amylose and synthetic polymers such as poly(L-lactide) (PLLA), which was achieved by the phosphorylase-catalyzed enzymatic polymerization of α -D-Glucose 1-phosphate salt (G-1-P) using a maltooligosaccharide primer in the presence of guest polymers. The representation of this reaction system is similar to the way that vines of plants grow twining around a rod. Accordingly, we have proposed that this polymerization method for the preparation of amylose-polymer inclusion complexes is named “vine-twining polymerization” [1]-[3]. In this study, we performed vine-twining polymerization using maltooligosaccharide-functionalized poly(L-lactide), which was a primer-guest conjugate (Figure 1). The XRD, ¹H NMR, and GPC results of product indicated that the elongated amylose chain included PLLA each other to produce the inclusion supramolecular polymer [4].

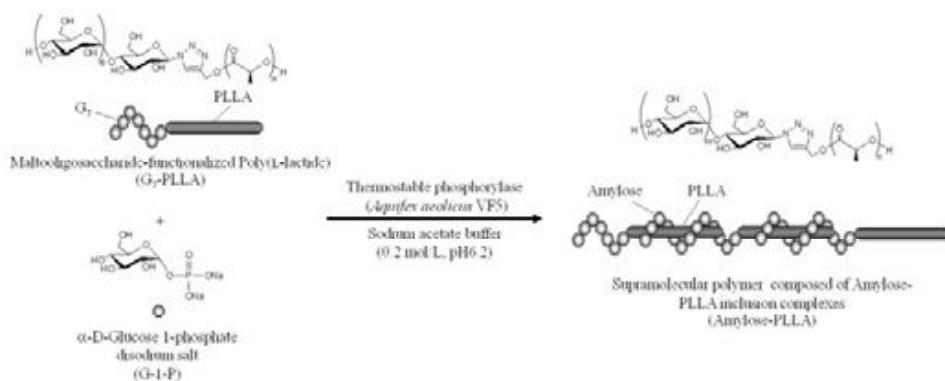


Figure 1 Preparation of supramolecular polymer by vine-twining polymerization using G₇-PLLA

References

- 1) J. Kadokawa, *Polymers* 2012, 4, 116.
- 2) Kadokawa, *Biomolecules* 2013, 3, 369.
- 3) Y. Kaneko, K. Ueno, T. Yui, K. Nakahara, J. Kadokawa, *Macromol. Biosci.* 2011, 11, 1407.
- 4) T. Tanaka, S. Sasayama, S. Nomura, K. Yamamoto, Y. Kimura, J. Kadokawa, *Macromol. Chem. Phys.* 2013, 214, 2829.

Preparation of Carboxymethyl Cellulose/Chitin Nanofiber Composite Films

Daisuke HATANAKA, Kazuya YAMAMOTO, Jun-ichi KADOKAWA

Graduate School of Science and Engineering, Kagoshima University

Abstract

Carboxymethyl cellulose (CMC), an acidic polysaccharide, is one of the widely applied cellulose derivatives. On the other hand, chitin, an aminopolysaccharide, can be considered as a basic polysaccharide because of the presence of amino groups due to deacetylation of a few percents of acetamido groups. We already reported that a dispersion of chitin nanofibers (CNF) was obtained by regeneration technique from a chitin/1-allyl-3-methylimidazolium bromide ion gel using methanol [1-3]. To produce useful composite materials from these acidic and basic polysaccharides, in this study, we performed the preparation of CMC/CNF composite films by electrostatic interaction [4]. A water insoluble CMC film was first prepared by the treatment of a CMC sodium salt aqueous solution with the cation-exchange resin, followed by drying. The preparation of CMC/CNF composite films was performed by immersing the CMC films in the CNF dispersions with different contents. By the weight measurements of the resulting films, it was confirmed that the amounts of the absorbed CNF per unit area on the CMC films increased with increasing the CNF contents. The SEM images showed that CNF were absorbed on the CMC films, giving rise to the composite films (Figure). The composite films exhibited better mechanical property than that of the CMC film.

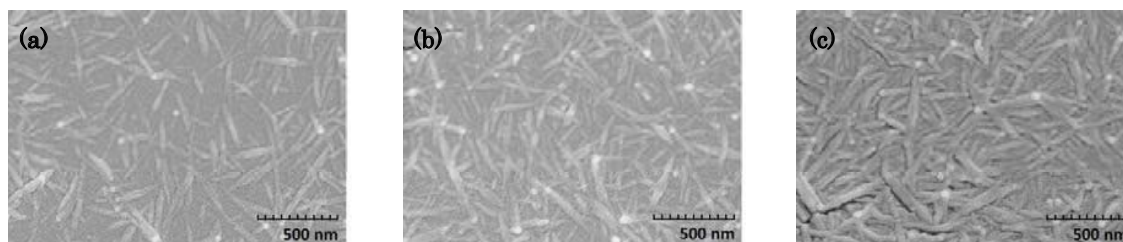


Figure. SEM images of CMC/CNF composite films prepared by using CNF dispersions ((a) 0.75 mg/mL, (b) 1.5 mg/mL, (c) 3.0 mg/mL)

References

1. K. Prasad, M. Murakami, Y. Kaneko, A. Takada, Y. Nakamura, J. Kadokawa, *Int. J. Biol. Macromol.*, 45, 221 (2009).
2. J. Kadokawa, A. Takegawa, S. Mine, K. Prasad, *Carbohydr. Polym.*, 84, 1408 (2011).
3. R. Tajiri, T. Setoguchi, S. Wakizono, K. Yamamoto, and J. Kadokawa, *J. Biobased Mater. Bioenergy*, 7, 655 (2013).
4. D. Hatanaka, K. Yamamoto, and J. Kadokawa, *Int. J. Biol. Macromol.*, 69, 35 (2014).

Preparation of Imidazolium Group-containing Silsesquioxane Indicating Ionic Liquid Nature

Takuhiro ISHII,¹ Toshiaki ENOKI,² Tomonobu MIZUMO,² Joji OHSHITA,² and Yoshiro KANEKO¹

¹Graduate School of Science and Engineering, Kagoshima University

²Graduate School of Engineering, Hiroshima University

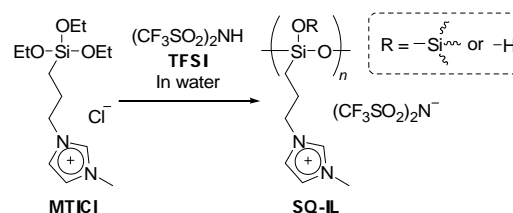
Abstract

Ionic liquids have been widely studied for their remarkable potential. However, little has been reported regarding the preparation of ionic liquids containing inorganic frameworks¹. Recently, we successfully prepared a silsesquioxane (SQ) indicating ionic liquid nature by sol-gel reaction of quaternary ammonium group-containing organotrialkoxysilane using aqueous bis(trifluoromethanesulfonyl)imide (TFSI)².

In this study, a new SQ ionic liquid (SQ-IL) was prepared by the sol-gel reaction of imidazolium group-containing organotrialkoxysilane monomer (MTICl) in aqueous TFSI. The DSC thermogram of SQ-IL exhibited the endotherm peak at -25 °C due to T_g and SQ-IL showed fluidity under 0 °C, *i.e.* room temperature ionic liquid. We also investigated the correlation between the structure of silsesquioxane and ionic liquid nature.

References

- 1) K. Tanaka, F. Ishiguro, and Y. Chujo, *J. Am. Chem. Soc.*, 2010, 132, 17649.
- 2) T. Ishii, T. Mizumo, and Y. Kaneko, *Bull. Chem. Soc. Jpn.*, 2014, 87, 155.



Scheme 1. Preparation of SQ-IL by hydrolytic condensation (sol-gel reaction) of MTICl using TFSI aq.

Preparation of Hydrophobic Polysilsesquioxanes and Their Hybridization with Organic Polymers

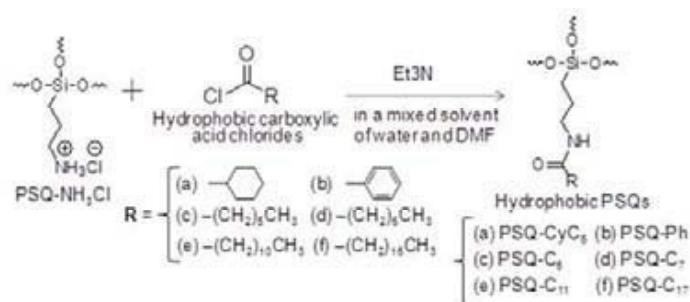
Hitomi IMAMURA,¹ Takuo SUGIOKA,² Yasutaka SUMIDA,² and Yoshiro KANEKO¹

¹ Graduate School of Science and Engineering, Kagoshima University
² Nippon Shokubai

Abstract

Silsesquioxanes (SQs) have attracted much attention in the research fields of organic-inorganic hybrid materials. However, the soluble polySQs (PSQs) with regular structures have only been obtained in the limited cases. So far, we reported that ammonium group-containing rod-like (ladder-like) PSQs with the hexagonally stacked structure (PSQ-NH₃Cl) was successfully prepared by the sol-gel reaction of 3-aminopropyltrimethoxysilane (APTAMOS) using aqueous strong acid such as HCl¹⁾.

In this study, we synthesized hydrophobic PSQs by the reaction of PSQ-NH₃Cl with various hydrophobic carboxylic acid chlorides in the presence of triethylamine in a mixed solvent of water and DMF (Scheme 1). In addition, we investigated the preparation of the hybrid films of organic polymer, *i.e.* polystyrene and polymethylmethacrylate, with the resulting hydrophobic PSQs.



Scheme 1. Synthesis of hydrophobic PSQs.

Reference

1) Y. Kaneko et al., Chem. Mater. 2004, 16, 3417.; Polymer 2005, 46, 1828.; Z. Kristallogr. 2007, 222, 656.; Kobunshi Ronbunshu (Japanese) 2010, 67, 280.; Int. J. Polym. Sci. 2012, 684278.

Preparation of Water-Soluble Chiral Ladder-like Polysilsesquioxanes and Their Chiral Induction Behavior into Dye Compounds

Shota KINOSHITA,¹ Hisako SATO,² and Yoshiro KANEKO¹

¹ Graduate School of Science and Engineering, Kagoshima University

² Graduate School of Science and Engineering, Ehime University

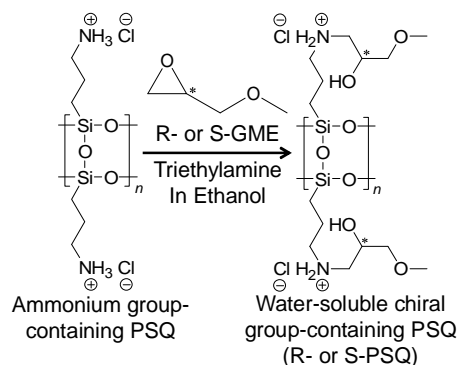
Abstract

Hybrids formed by noncovalent interactions between photofunctional compounds and chiral molecules have attracted considerable attention because of their potential application in circularly polarized luminescent materials. However, there have been few reports regarding hybridization using inorganic compounds such as siloxane-based materials as chiral inductors. So far, we have reported the preparation of ladder-like polysilsesquioxanes (PSQs) containing chiral and ammonium side-chain groups and the investigation of their chiral induction behavior into dye compounds¹. However, these PSQs were insoluble in water.

In this study, therefore, we prepared water-soluble ladder-like PSQs containing chiral groups by reaction of PSQ containing ammonium groups² with chiral glycidyl methyl ethers (GMEs). In addition, it was found that the chirality was induced from the chiral PSQs into dye compound in water.

References

1. Y. Kaneko et al., *J. Mater. Chem.*, 2009, 19, 7106.; *J. Mater. Chem.*, 2011, 21, 16638.; *J. Nanosci. Nanotechnol.*, 2013, 13, 3074.
2. Y. Kaneko et al., *Chem. Mater.*, 2004, 16, 3417.; *Int. J. Polym. Sci.*, 2012, 684278.



Scheme 1. Preparation of water-soluble ladder-like PSQs containing chiral groups (R- and S-PSQs).

One-step Preparation of Soluble Polymer Composed of POSS Units

Takahiro TOKUNAGA,¹ Sayako KOGE,² Tomonobu MIZUMO,² Joji OHSHITA,²
Yoshiro KANEKO¹

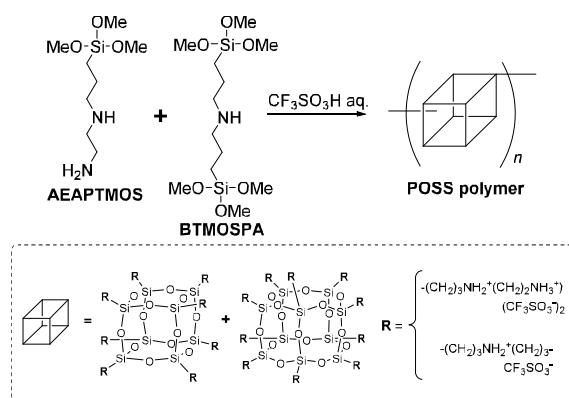
¹ Graduate School of Science and Engineering, Kagoshima University

² Graduate School of Engineering, Hiroshima University

Abstract

Cage-like oligosilsesquioxane (POSS)-containing polymers have attracted much attention because they have potentials to exhibit superior thermal and mechanical stabilities due to siloxane (Si-O-Si) bond frameworks. On the other hands, recently, we reported the facile preparation of POSS compounds by the hydrolytic condensation of amino group-containing organotrialkoxysilanes using superacid such as CF₃SO₃H aqueous solution.^{1), 2)} In this study, we found that the soluble polymer composed of POSS units (POSS polymer) was successfully prepared in one-step

by hydrolytic condensation of the mixture of two types of amino group-containing organotrialkoxysilanes, 3-(2-aminoethylamino)propyltrimethoxysilane (AEAPT MOS) as a raw material of POSS and bis[3-(trimethoxysilyl)propyl]amine (BTMOSPA) as a cross-linker, using aqueous CF₃SO₃H as a catalyst (Scheme 1).



Scheme 1. Preparation of Soluble Polymer Composed POSS Units.

References

- 1) Y. Kaneko, M. Shoiriki, and T. Mizumo, *J. Mater. Chem.*, 2012, 22, 14475.
- 2) T. Tokunaga, M. Shoiriki, T. Mizumo, and Y. Kaneko, *J. Mater. Chem. C*, 2014, 2, 2496.

Preparation of Phthalimido Group-containing Ladder-like Polysilsesquioxane

Shunya MIYAUCHI,¹ Takuo SUGIOKA,² Yasutaka SUMIDA,²
Toshiaki ENOKI,³ Joji OHSHITA,³ and Yoshiro KANEKO¹

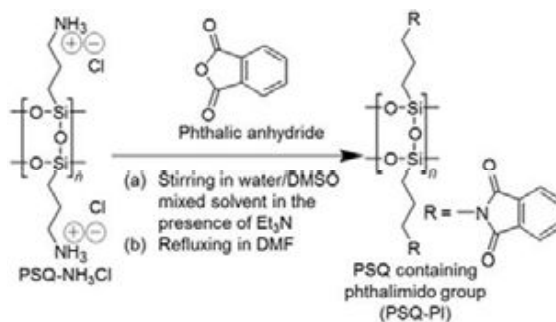
¹Graduate School of Science and Engineering, Kagoshima University

²Nippon Shokubai

³Graduate School of Engineering, Hiroshima University

Abstract

We prepared a polysilsesquioxane (PSQ) containing phthalimido groups (PSQ-PI) by reaction of phthalic anhydride with amino group-containing ladder-like PSQ, which was prepared by the hydrolytic polycondensation of 3-aminopropyltrimethoxysilane monomer using HCl aqueous solution as a catalyst (Scheme 1)¹⁾. PSQ-PI was soluble in chloroform, DMF, and DMSO. In addition, this polymer showed a high thermal stability, which was confirmed by TGA.



Scheme 1. Preparation of PSQ-PI.

Reference

1) Y. Kaneko et al., Chem. Mater., 2004, 16, 3417.; Polymer, 2005, 46, 1828.; Z. Kristallogr., 2007, 222, 656.; Kobunshi Ronbunshu (Japanese), 2010, 67, 280.; Int. J. Polym. Sci., 2012, 684278.

Application of Wavelet Transform for Analysis of Defluidization Caused by the Reaction Involving Gas-Volume Reduction

Norihiro TANAKA¹, Takami KAI¹, Kei MIZUTA¹, Tsutomu NAKAZATO¹
And Mitsuyuki NAKAJIMA²

¹ Graduate School of Science and Engineering, Kagoshima University

² IHI Plant Engineering Corporation

Abstract

Fluidized beds have been used as catalytic reactors since the development of the fluid catalytic cracking process. Although good fluidization establishment is necessary for the stable operation of a fluidized catalyst bed, the bed is disturbed by the defluidization that occurs when the reaction performed in the bed is accompanied by a decrease in the gas volume [1]. Some methods have been proposed to prevent the defluidization caused by the decrease in gas volume [2, 3]. However, even if these methods are utilized for these types of reactions, defluidization is not perfectly suppressed. In this paper, we studied the effectiveness of pressure fluctuation signals to detect defluidization causing conditions when CO₂ methanation was performed in a fluidized catalyst bed. In addition, we studied whether the onset of defluidization itself could be predicted. For these purposes, continuous wavelet transfer (CWT) analysis was performed to determine the frequency characteristics of pressure drop fluctuations. On the basis of the results, the autocorrelation function was used to identify the fluidization conditions.

The occurrence frequency of channeling and bed lifting depended on the reaction conditions. Even when the conditions were in the defluidization region [4], the bed was observed to be fully fluidized most of the time. We investigated the characteristics in this pseudo-stable region. The pressure drop was stable in this region, and the fluctuation amplitudes were not large as compared with the results in the good fluidization region. However, a comparison among the CWT analysis results clearly reveals that the intensity above 10 Hz decreased when the conditions were in the defluidization region.

The pattern of the autocorrelation function was affected by the fluidization region. When the conditions were in the good fluidization region, the autocorrelation function changed periodically and the peak value gradually decreased with lag time. The dominant frequency was approximately 14 Hz. When the conditions were in the defluidization region. Because the maximum peak values decreased, the periodicity of the fluctuations was lowered. In addition, the dominant frequency was slightly lower than that in the good fluidization region. Generally, the dominant frequency of pressure fluctuations is related to the bubble frequency. High frequency of pressure fluctuations implies the existence of small bubbles [5]. Therefore, bubble size was probably increased in the defluidization region. Even when the bed appears to be fully fluidized according to our visual observation, the peak values of the autocorrelation functions decreased and/or the dominant frequency was lowered in the defluidization region.

When the bed was fully fluidized in the defluidization region, the fluidization quality decreased because the emulsion phase expansion was reduced by the decrease in gas volume due to the reaction. Generally, the reactant concentration is high around bubbles and accordingly the reaction rate is high in this zone. Therefore, the voidage distribution in the emulsion phase was affected by the movement of bubbles. This probably influenced the frequency and the periodicity of the pressure drop fluctuations.

Literature Cited

- 1) Kai, T., S. Furusaki, Chem. Eng. Sci. 42 335–339 (1987).
- 2) Kai, T., M. Furukawa, K. Toriyama, T. Nakazato, M. Nakajima, J. Chem. Eng. Japan 42, 733–738 (2009).
- 3) Kai, T., A. Matsumura, T. Nakazato, M. Nakajima, Chemical Engineering Journal 215-216, 671–677 (2013).
- 4) Kai, T., K. Toriyama, K. Nishie, T. Takahashi, M. Nakajima, AIChE J. 52 3210–3215 (2006).
- 5) Sheikhi A., R. Sotudeh-Gharebagh, N. Mostoufi, R. Zarghami, Powder Technol. 235 787–796 (2013).

Production of Biodiesel without By-Produced Glycerol from Transesterification of Canola Oils

Goon Lum MAK¹, Takami KAI¹, Tsutomu NAKAZATO¹, Saki INAMINE¹,
Hirokazu TAKANASHI¹

¹ Graduate School of Science and Engineering, Kagoshima University

Abstract

Biodiesel is produced by transesterification of fats and methanol. This fuel has attracted researchers' attention for the reduction of fossil fuel consumption. However, glycerol is by-produced during the reaction. Since the methyl ester phase and glycerol phase mutually cannot solve each other, methyl esters can be separated using difference in specific gravity. The amount of the by-produced glycerol has inevitably increased with the increase of the biodiesel production. Consequently, the overproduction of glycerol has lowered the price of purified glycerol. Previously, some studies proved that the replacement of methanol with dimethyl carbonate (DMC) formed no glycerol [1]. Some of the studies using alkali catalysts required excessive amount of catalyst and dimethyl carbonate [2]. We modified the method of catalyst preparation when sodium methoxide was used in our previous study [3]. In this study, we investigated better method to improve the efficiency of the reaction. In the investigation, we realized some details happening during reaction, and this may help to improve efficiency of the reaction under mild condition in future.

For this study canola oil and DMC as reactant, and sodium methoxide (NaOCH₃) as a heterogeneous catalyst were used. Reaction was performed in a round-bottomed glass flask and a Teflon tube reactor. To enhance the catalytic activity, we have prepared the catalyst by crystallization [3]. Samples were analyzed using high-performed liquid chromatography.

The wave of ultrasonic could shake the radiated molecules. So in theoretically, preparing NaOCH₃ catalyst under ultrasonic environment may avoid catalyst grow bigger during recrystallization process. However, in the experiment under ultrasonic environment, any improvement was not observed, and the conversion was the same with the result of our previous study.

When reaction performed in round-bottomed glass flask, DMC will evaporate into the gas phase even under the boiling point (90 °C). This caused the decrease in DMC concentration in the liquid phase, and the reduction of triglyceride conversion. To decrease evaporation of DMC during reaction, at initial stage of reaction set in lower temperature by temperature controller. The experimental result shows that those conversion was around 90–92%, compare these with previous study in same condition, it had a bit improvement around 2–3%.

We used a tubular reactor to completely avoid evaporation of DMC. The length of the tube was 10 m. A round-bottomed glass flask was used as a reactant reservoir. The reactant mixture containing catalyst was supplied by a micro tube pump. Conversion of the product was around 72%. The low conversion caused by duration of heating was too short and laminar flow made agglomerated catalyst stick together after reaction. Analysis of the brownish part in the tube by HPLC showed that this phase contained the high concentration of glycerol dicarbonate. The product is considered to be the material which reduced NaOCH₃ catalyst activity and caused the catalyst agglomeration.

References

- 1) Fabbri, D., Bevoni, V., Notari, M., Rivetti, F., *Fuel*, 86, 690–697 (2007).
- 2) Zhang, L.P., B.Y., Sheng, Z., Xin, Q., Liu, S.Z., Sun, *Bioresource Technol.*, 101, 8144–8150 (2010).
- 3) Kai, T., Mak, G.L., Wada, S., *Bioresource Technol.*, 163, 360–366 (2014).

Effect of optical flow in the entire visual field on attentional blink

Shinya TAKAGAWA¹, Ken KIHARA¹, Sakuichi OHTSUKA¹

¹Graduate School of Science and Engineering, Kagoshima University

Abstract

Recently popularized see-through augmented-reality (AR) systems produce optical flow in the entire visual field. It is possible that this optical flow interferes with the visual information given by the AR system. Previous studies have shown that the optical flow generated in a limited background affects the visual attention when stimuli are presented successively at the central visual field [1]. However, the relationship between the optical flow of the entire field and the visual attention is still unclear. To address this issue, we used the attentional blink (AB) phenomenon [2]; with two targets embedded in a rapid stream of stimuli, identification of the second target becomes difficult if it occurs 200-500 ms after the first target (Fig.1A, 1B). We examined the effect of the optical flow induced by moving dots scattered across the entire visual field on AB (Fig.1C). The characteristics of the optical flow were varied by changing the direction, speed and number of moving dots (Fig.1D). The results of experiments revealed that there were no specific differences in AB size regardless of optical flow conditions (Fig. 1E). These results suggest that optical flow in the entire field may not have a significant impact on the visual attention in the environment of see-through AR.

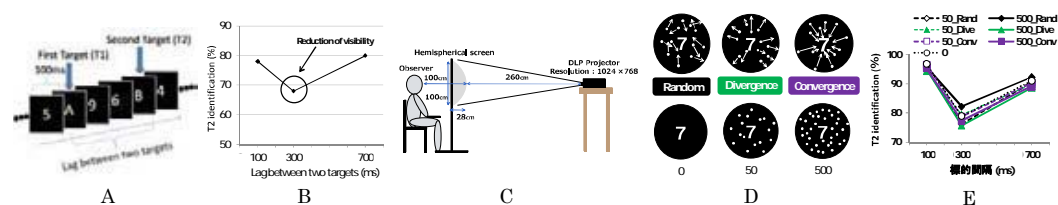


Figure 1. Figures used in the poster.

References

- 1) Arend, I., Stephen, J., & Shapiro, K-L. (2006). Task-irrelevant visual motion and flicker attenuate the attentional blink. *Psychonomic Bulletin & Review*, 13, 600-607.
- 2) Raymond, J-E., Shapiro, K-L., & Arnell, K-M. (1992). Temporary Suppression of Visual Processing in an RSVP Task: An Attentional Blink? *Journal of Experimental Psychology*, 18, 849-860.

Adding blue or yellow sector onto Benham's top

Chiemi MIYATA¹ Kaori SHOJI¹ Ken KIHARA¹ Sakuichi OHTSUKA¹
and Hiroshi ONO²

¹Graduate School of Science and Engineering, Kagoshima University
²Department of Psychology, York University, Toronto, Canada

Abstract

Schramme showed that the S and (M+L) cone opponent color mechanism is responsible for seeing a yellowish apparent color at the transition of black to white and bluish one at the transition of white to black when Benham's top is spinning [1]. To better understand this mechanism, we investigated the effects of adding blue or yellow sector at the transition edges (Fig.1A). Nine observers who had normal color vision were asked to judge whether the bluish tint component was greater in the experimental stimulus than in the spinning Benham's top. We found that (1) the stimulus with yellow (or blue) colored sectors at black to white (or white to black) transitions induced bluish (or yellowish) color at both transitions, and (2) the stimulus with blue (or yellow) colored sectors at black to white (or white to black) transitions induced highly saturated bluish-color at the white to black edges but induced same amount of yellowish-colored arcs at the black to white edges compared with that of normal Benham's top (Fig.1B). (1) and (2) together showed that yellow sector affects percepts at both transitions of black to white and white to black, but the blue sector affect only at the transition of white to black(Fig.1C).

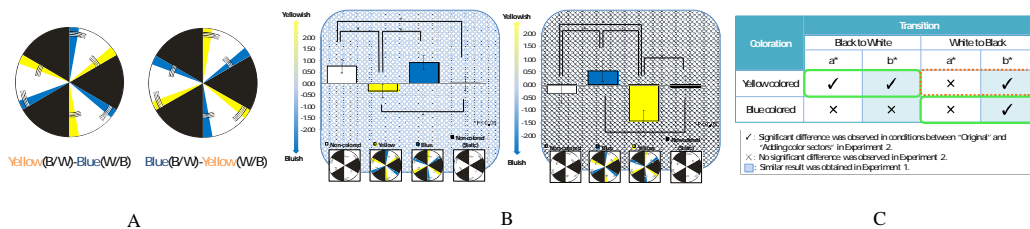


Figure.1 Figures used in the poster.

References

- 1) C. von Campenhausen, et al., "100 years of Benham's top in colour science," Perception, vol. 24, no. 6, pp. 695 - 717, 1995.